Nitrogen Fixation by Nitrogenases: A Quantum Chemical Study

Per E. M. Siegbahn* and Joakim Westerberg

Department of Physics, Stockholm University, Box 6730, S-113 85 Stockholm, Sweden

Mats Svensson

Department of Chemistry, Organic Chemistry, Royal Institute of Technology, S-100 44 Stockholm, Sweden

Robert H. Crabtree

Chemistry Department, Yale University, 225 Prospect Street, New Haven, Connecticut 06520-8107

Received: July 8, 1997; In Final Form: December 3, 1997

The mechanism of ammonia formation by nitrogenase has been studied using the hybrid density functional method B3LYP with large basis sets. Most of the results were obtained with a simple iron dimer model, but a few calculations were also done for larger models, the largest one containing eight iron atoms. The model clusters were in general chosen to have a net neutral ionic charge with the iron atoms in the low Fe(II) oxidation state with ferromagnetically coupled spins. In a key result we find that placing a hydrogen atom on a bridging sulfur dramatically changes the affinity of the cluster for N_2. In the dimer model without this hydrogen atom, N_2 forms only a weak end-on bond to one of the iron atoms, but with the hydrogen atom present N_2 becomes strongly activated in a bridging coordination. The effect of the hydrogen atom can be described as a local promotion effect reducing the Fe_2(II,II) system to an Fe_2(I,II) set. A very similar promotion effect is seen also for the larger clusters. Another interesting effect noted for the Fe_8 cluster is that a cavity between the cubanes in the cluster can be opened by reducing the cluster with two hydrogen atoms on bridging sulfurs. Coupled electron and proton transfer and energetic aspects are emphasized. Most steps of ammonia formation are shown to lead to H atom addition energies in the range 50−60 kcal/mol, which is argued to be optimal for the function of nitrogenase.

I. Introduction

Nitrogenase (N_2-ase) is an enzyme widely distributed among bacteria and is key to the fixation of N_2 in the terrestrial nitrogen cycle with an estimated annual global ammonia production of 1.7×10^{11} kg.[1−7] N_2-ase is able to reduce N_2 to ammonia via eq 1 using a relatively mild source of electrons—a reduced ferredoxin in vivo and sodium dithionite in vitro—together with protons from the medium.

$$8e^- + 8H^+ + N_2 \rightarrow 2NH_3 + H_2 \qquad (1)$$

A notable feature of the stoichiometry of the enzyme is the apparent requirement for the production of at least one H_2 molecule per N_2 molecule reduced, suggesting that H_2 evolution may have some essential role in the chemistry.[8] The first nitrogenases to be isolated from bacteria such as *Azotobacter vinelandii* and *Clostridium pasteurianum* had Mo, Fe, and S^{2-} as inorganic constituents,[9,10] but later "alternative" forms were discovered with V, Fe, and S^{2-} or even with Fe and S^{2-} alone as constituents.[5,11,12] In what follows we restrict our attention to the molybdenum-containing protein because it is for this case that crystal structures have been solved.[13,14] Early work showed that the enzyme consists of a ca. 60-kD Fe-containing protein, which provides the electrons required in eq 1, and a ca. 220-kD protein-containing Fe, Mo, and inorganic sulfide that binds and reduces N_2. The Fe protein has a binding site for MgATP which leads to a conformational change causing binding to the MoFe protein and to a 120-mV increase in the reducing power of the Fe protein, the former certainly and the latter possibly required for electron transfer to take place. In the course of the catalytic cycle, two MgATP molecules are normally hydrolyzed to MgADP per electron transferred from the Fe to the MoFe protein. The hydrolysis may or may not be coupled to the electron transfer, possibly providing energy to drive the electron transfer.[4] Turning now to the MoFe protein, an air-sensitive Fe−Mo−S-containing cofactor (FeMoco),[15] extracted from the MoFe protein, was found to reconstitute catalytic activity in the apoenzyme, although no combination of inorganic reagents could do so. This suggested that an Fe−Mo−S cluster of an unusual type (M center) might be the key active site component. Later work identified several genes[5] involved in FeMoco synthesis including one for homocitrate synthesis, which led to the recognition that homocitrate acts as a ligand in FeMoco. Altering this ligand affects the reduction rate and specificity. In the dithionite-reduced form of the enzyme, the FeMoco cluster is in the $S = 3/2$ spin state, but N_2 is believed to bind only in some more reduced state. Apart from FeMoco, the MoFe protein also contains an Fe_8S_8 cofactor (the P cluster) of a very unusual structure, but which is believed to be involved in electron transfer and not substrate binding. A number of alternative substrates and/or competitive inhibitors, such as acetonitrile, methylisonitrile, acetylene, N_2O, CO, and CN^- ion presumably bind to FeMoco. Kinetic work by Thorneley and Lowe[16] has led to a proposed scheme involving 10 intermediates in which N_2 only binds after cluster reduction by three or four electrons. In essentially all the reductions catalyzed by N_2-

S1089-5647(97)02207-4 CCC: $15.00
Published on Web 02/04/1998

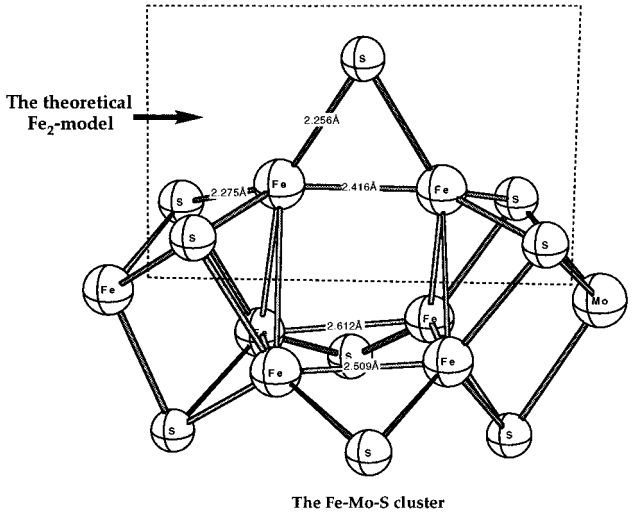

Figure 1. Experimental structure[13] for the FeMo cofactor, with a dashed line showing a position where the present dimer model could fit.

ase, with N_2 or with alternative substrates, an equal number of protons and electrons are transferred to the substrate, so the enzyme is acting as a net hydrogen atom donor, suggesting that proton and electron transfer may be closely coupled. With some substrates there is an initial burst of about one H_2 molecule per Mo, which could be due to the substrate displacing H_2 on binding.[17] The crystallographic work of the Rees and Bolin groups[13,14,18] has made the present study possible by providing a structural basis for discussing the N_2-ase mechanism. In particular it has revealed the very surprising structure of FeMoco shown in Figure 1. The results show that the Mo, long suspected to be the N_2-binding site, is in fact six-coordinate and therefore possibly coordinatively saturated (although seven-, eight- and even[19] nine-coordinate Mo complexes are known) at least in the state of the enzyme that was crystallized. In contrast, six of the seven irons appear to be three-coordinate. Of course, the presence of light ligands such as H cannot be excluded, but the abnormally low apparent coordination number found for these irons certainly make them a likely site for substrate binding. The definitive characterization of an all-iron N_2-ase[5] is also consistent with this idea. The crystal structure of Mo−N_2-ase also shows[20] that a variety of potentially hydrogen-bonding groups, such as the homocitrate, His 195, Arg 359, and Arg 96, are located around the FeMoco cluster and could play a role in proton transfer to the cluster. The latter process may well be coupled with electron transfer to give a net hydrogen atom transfer to the FeMoco cluster; see below.

Because of the size of the FeMo cofactor, so far mainly simple semiempirical methods have been used to study this system theoretically. Deng and Hoffmann[21] used the extended Hückel method and concluded that metal−metal bonding in the cofactor is quite important. Several N_2 coordination modes were considered. Stavrev and Zerner[22] used the INDO (intermediate neglect of differential overlap) and found that N_2 preferably binds within the cluster. Even though the INDO method is known to exaggerate binding energies, the binding energy obtained of nearly 150 kcal/mol is extraordinarily large. The only previous density functional theory (DFT) study of nitrogenase is a very recent investigation by Dance.[23] Gradient corrections of the density were used, but Hartree−Fock exchange was not included, and the entire cofactor was considered. The optimal geometry found for N_2 was quite asymmetric, with both nitrogens mainly bound to one of the two incomplete cubane clusters of the cofactor.

The challenge of finding the molecular mechanism for N_2 reduction in N_2-ase has continued to be elusive in spite intense study. We cannot expect our contribution, described in this paper, to provide more than a preliminary working hypothesis, but we believe it provides testable ideas for future study. In this study, we use quantum chemical methods to study some of the details of ammonia formation. The use of high accuracy quantum chemical methods in the field of biochemistry involving transition metals is very new. In general, for standard ab initio methods the systems are simply too big. DFT methods have for some time had the capacity of treating large enough systems, but the accuracy has been questionable. Recent work in this area[24] incorporating gradient corrections of the density and Hartree−Fock exchange in a scheme parametrized against experiments has changed the situation dramatically. The accuracy of these types of hybrid methods is now almost of the same level as that obtained by the most advanced ab initio methods obtainable for small systems.[25] The use of empirical parameters has not had any significant effect on the range of applicability of these methods. Since only a few (in the present case three) parameters selected on physical grounds are used, the methods are equally applicable for systems for which the parameters have not been fitted, such as for transition metal complexes.[26] This is unlike the situation for the earlier type of semiempirical schemes where many more parameters were used. The present DFT methods have previously been proven useful for biochemical systems. In an application to the mechanism for methane activation by methane monooxygenase (MMO), an unusual distorted structure was predicted for the key active complex denoted compound **Q**,[27] which later proved to be identical with the model suggested on the basis of recent EXAFS measurements.[28] The energetics obtained for the methane reaction is also in very good agreement with available experimental information. Exactly the same type of methods and procedures were used in the MMO study as in the present study of N_2-ase.

Although the methods used here are capable of treating relatively large systems, even a single calculation on a system as large as the FeMo cofactor is a challenge. A few such calculations will be presented here, but the main body of results have to be obtained on smaller models. Otherwise, the number of calculations required to properly test a mechanistic hypothesis cannot be performed. The models used in the present study are built on two simplifying principles. First, charge-neutrality is maintained as far as possible. This is in general a reasonable assumption for proteins, which have rather low dielectric constants. It should be emphasized that this type of model is still consistent with local charge fluctuations, such as proton transfer between two neighboring sites and proton exchange with the solvent. The second assumption is that proton transfer (PT) and electron transfer (ET) are strongly coupled, as is consistent with the charge-neutrality assumption. The ultimate limit of strongly coupled PT and ET is hydrogen atom transfer (HAT), which has recently been shown to be a good model for the strongly coupled PT and ET processes occurring in ribonucleotide reductase (RNR).[29] In prior quantum chemical model studies, two different mechanisms of HAT between amino acids were demonstrated, proton-governed hydrogen transfer (PGHT) and overlap-governed hydrogen transfer (OGHT). In PGHT, a proton moves first to set up a potential in which the electron can then also move. In OGHT, the system is set up in a way such that the critical orbitals overlap, allowing a proton and an electron transfer to occur simultaneously but by different paths. In both mechanisms, at the end of each step an entire hydrogen

atom has moved. A key point is that the charge separation is kept minimal in this transfer.

Strong coupling between PT and ET in N_2-ase has previously been advocated by several workers. In a recent review on N_2-ase Thorneley says that "the importance of the coupling of proton and electron transfers cannot be overemphasized".[30] He adds that a probable key role for ATP hydrolysis is to synchronize electron and proton transfer and that the role of the P-clusters could be control of both electron donation to and protonation of the FeMoco substrate reduction site. In an even more recent review,[4] Burgess and Lowe emphasize the importance of a coupling between ET and PT, as follows: "it is possible that this type of sequential electron/proton transfer (i.e., net hydrogen atom transfer) occurs for the FeMo cofactor site of nitrogenase". The models used in the present study rely heavily on this picture of a very strong coupling between ET and PT.

Use of the HAT picture is the first characteristic feature of the present study on N_2-ase. The second is the relatively small size of the systems used as models in most cases. The choice of a small model is obviously partly dictated by the size of the calculations, but these models are also used on the basis of some initial experience for the present system. It is today actually possible to treat systems almost as large as the FeMo cofactor. However, the initial results of using a quite realistic model containing eight iron atoms and placing N_2 at different sites of this cluster were quite discouraging and did not lead to any progress on the mechanism of N_2-ase. The main reason for this was that only very few calculations could be afforded and so the flexibility and variations of the models used were therefore severely limited. A much simpler model containing only two iron atoms was much more successful in elucidating probable mechanisms. The present paper will mainly describe the results obtained using this simple model. Toward the end of the paper, results using more realistic models are also described testing the mechanisms obtained using the smaller model.

II. Computational Details

The calculations were performed in two steps. First, an optimization of the geometry was performed using the B3LYP method.[24] Double-zeta basis sets were used in this step. In the second step the energy was evaluated for the optimized geometry using very large basis sets including diffuse functions and with two polarization functions on each atom. The final energy evaluation was also performed at the B3LYP level. All calculations were made using the Gaussian-94 program.[31]

The B3LYP functional can be written as,[24,32]

$$F^{\mathrm{B3LYP}} = (1-A)F_{\mathrm{x}}^{\mathrm{Slater}} + AF_{\mathrm{x}}^{\mathrm{HF}} + BF_{\mathrm{x}}^{\mathrm{Becke}} + CF_{\mathrm{c}}^{\mathrm{LYP}} + (1-C)F_{\mathrm{c}}^{\mathrm{VWN}}$$

where $F_{\mathrm{x}}^{\mathrm{Slater}}$ is the Slater exchange, $F_{\mathrm{x}}^{\mathrm{HF}}$ is the Hartree−Fock exchange, $F_{\mathrm{x}}^{\mathrm{Becke}}$ is the gradient part of the exchange functional of Becke,[24] $F_{\mathrm{c}}^{\mathrm{LYP}}$ is the correlation functional of Lee, Yang, and Parr,[33] and $F_{\mathrm{c}}^{\mathrm{VWN}}$ is the correlation functional of Vosko, Wilk, and Nusair.[34] *A*, *B*, and *C* are the coefficients determined by Becke[24] using a fit to experimental heats of formation, but Becke did not use $F_{\mathrm{c}}^{\mathrm{VWN}}$ and $F_{\mathrm{c}}^{\mathrm{LYP}}$ in the expression above when the coefficients were determined, but used the correlation functionals of Perdew and Wang instead.[35]

The B3LYP energy calculations were for all the iron dimer models made using the large 6-311+G(2d,2p) basis sets in the Gaussian-94 program. This basis set has two sets of polarization functions on all atoms including two f-sets on the metals and also diffuse functions. In the B3LYP geometry optimizations a much smaller basis set, the LANL2DZ set of the Gaussian-94 program, was used in most cases. For the iron atoms this means that a nonrelativistic ECP according to Hay and Wadt[36] was used. The metal valence basis set used in connection with this ECP is essentially of double-zeta quality. The sulfur atoms also have an ECP description, and the rest of the atoms are described by standard double-zeta basis sets. A few exceptions to this general recipe for performing the calculations were made. First, in a few geometry optimizations the effects of d-functions on sulfur were tested. Secondly, for the largest systems studied here with up to eight iron atoms, no additional large basis set calculation could be afforded, so the energies discussed below are for the same basis set as was used for the geometry optimization. Whenever there has been a deviation from the general procedure for doing the calculations, this will be explicitly mentioned in the text below.

The computational model systems used in the present paper are quite large by quantum chemical standards. The calculations could still be successfully performed using very large basis sets and accurate methods, as described above. However, the calculations of accurate Hessians turned out to be prohibitively expensive. Not only are the systems too big but it was also very difficult to obtain sufficient convergence for obtaining numerically reliable frequencies. Since the zero-point vibrational effects are expected to be small for the reactions involving the N_2-ase model, these were therefore simply assumed to be zero for these reactions. For the gas-phase reactions mentioned in the text as comparisons, zero-point effects where obtained at the B3LYP level using the LANL2DZ basis set.

III. Results and Discussion

Before the discussion of the results from the model calculations on N_2-ase starts, it is useful to consider some gas-phase results as a background. In N_2-ase the hydrogen atoms, or strongly coupled protons and electrons (see above), are supplied one at a time to the nitrogen molecule. The corresponding gas-phase energies, calculated at the same level as the other energies of this study, are the following:

$$N_2 + H \rightarrow N_2H, \quad \Delta E = 1.2 \text{ kcal/mol} \tag{2}$$

$$N_2H + H \rightarrow N_2H_2, \quad \Delta E = -60.7 \text{ kcal/mol} \tag{3}$$

$$N_2H_2 + H \rightarrow N_2H_3, \quad \Delta E = -50.3 \text{ kcal/mol} \tag{4}$$

$$N_2H_3 + H \rightarrow N_2H_4, \quad \Delta E = -75.9 \text{ kcal/mol} \tag{5}$$

$$N_2H_4 + H \rightarrow NH_2 + NH_3, \quad \Delta E = -45.0 \text{ kcal/mol} \tag{6}$$

$$NH_3 + NH_2 + H \rightarrow 2NH_3, \quad \Delta E = -101.0 \text{ kcal/mol} \tag{7}$$

A few important conclusions relevant for N_2-ase can be drawn from these energies. First, the most critical step is the addition of the first hydrogen to the triple bond of N_2, which is only thermoneutral in the gas phase. Secondly, since the average H-bond strength is 55.3 kcal/mol (exptl. 54.7 kcal/mol) from reactions 2−7, the cost of obtaining hydrogen atoms for the FeMo cofactor of N_2-ase should not be much higher than this value. In order not to waste unnecessary energy, the cost should not be much lower than 55 kcal/mol either. In an ideal situation, which probably has been achieved as closely as possible in N_2-ase by evolution, most steps of hydrogen addition to nitrogen should therefore lead to N−H bond strengths of 50−60 kcal/

mol. This is a very important guideline governing the present study. An exception to this rule could be the final H atom addition energies where ammonia is formed; see further below. To obtain hydrogen atoms at such a low cost as only 55 kcal/mol, N_2-ase has the Fe-protein which contains a reduced ferredoxin and where two MgATP are consumed for each hydrogen atom produced. To treat proton/electron transfer in this system, we consider that an H atom transport chain exists going from the Fe-protein via the P-cluster to the FeMo cofactor. A requirement for such a chain is that hydrogen atoms are not bound anywhere by significantly more than 55 kcal/mol, since they would otherwise never reach the FeMo cofactor. Preliminary calculations on models of the P-cluster indeed show that H-bond strengths of about this size are obtained, provided that the iron atoms in the P-cluster have low oxidation states, most of them Fe(II). For example, the calculated H atom bond strength to Fe_4S_4 with only Fe(II) atoms is 54.4 kcal/mol (obtained using the small basis set).

Although H_2 molecules are not used to supply H atoms in N_2-ase, it is still of interest to consider the reaction energy between N_2 and H_2. With a calculated binding energy of 103.8 kcal/mol for H_2 (exptl. 103.5 kcal/mol), the following is obtained:

$$N_2 + 3H_2 \rightarrow 2NH_3, \quad \Delta E = -19.9 \text{ kcal/mol} \qquad (8)$$

The experimental value for this reaction is −17.8 kcal/mol. It can be noted that the optimal cost of hydrogen atoms of about 55 kcal/mol is actually achieved fairly well by H_2 (52 kcal/mol per H atom). This is directly relevant for the industrial Haber−Bosch process where H_2 is used as hydrogen source. It is also relevant for N_2-ase in the sense that H_2 formation leads to a similar energy gain as the average step of the N_2-ase cycle. Unwanted formation of H_2 is for this reason a potential problem in ammonia synthesis, and an almost perfect fine-tuning of all steps in ammonia formation is therefore required. Still, for the FeMo cofactor a lower limit of one hydrogen molecule is produced in each ammonia cycle, as described in the Introduction. However, there is probably a reason for this which might be central for the ammonia synthesis, as will be described below.

a. Results for the Iron Dimer Model. As mentioned in the Introduction, the main reason for choosing an iron dimer model for the study of N_2-ase is that it allows a sufficient number of calculations to test different ideas of the mechanisms. The reason we did not start this investigation with an even simpler monomer model is that this does not allow the important case of a bridging N_2 to be tested. The goal of the dimer study is to provide sufficient insight to move to more realistic models later. In fact, even a totally negative result giving no indication of how ammonia is formed would be quite interesting since this would imply that at least three iron atoms are involved simultaneously in all key steps of the ammonia cycle. However, as it turns out, many qualitative aspects of ammonia formation can be understood on the basis of the dimer model, such as, for example, the role of hydrogen atoms in the cluster.

The following ideas and background were used to set up the starting iron dimer complex. First, there should be at least one bridging sulfur ligand. In the real FeMo cofactor pairs of iron atoms are connected both by one and two sulfur bridges. In the present dimer model, only one sulfur bridge was chosen since this should intuitively simplify possible N_2 bridging modes. Also, in the real FeMo cofactor these bridging sulfurs can be either μ^2- or μ^3-coordinated. Obviously, in a dimer model only μ^2-coordinated sulfurs can be tested, but in bigger models described in the next subsection μ^3-coordinated sulfurs will also be tested. It is probably highly significant that the iron atoms are only three-coordinate in the FeMo cofactor, and so three-coordination was therefore also chosen for the iron dimer model.

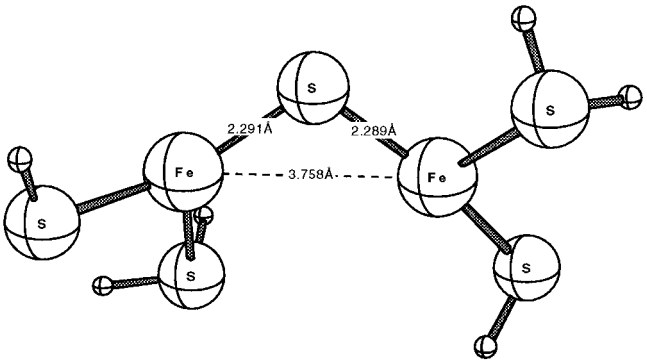

Figure 2. Fe_2(II,II) dimer model used as a starting point for the calculations.

A very important question in modeling the FeMo cofactor is what oxidation states should be used for the iron atoms. In the preliminary investigation of the neutral iron dimer model different oxidation states were modeled using the simplest possible sulfur-based ligands, which means using either SH or SH_2 ligands. As mentioned above, the iron atoms are kept three-coordinate and a single sulfur bridge is also included in the model. The criterion used to judge the suitability of a model is how strongly hydrogen atoms are bound to the ligands around iron. If a hydrogen atom can be bound to one of the sulfur ligands by significantly more than 55 kcal/mol (the average bond strength to nitrogen, see above), then this would not be a good model. A hydrogen atom travelling through the FeMo cofactor would then get permanently bound at this position and would not be able to travel further to reach the nitrogens. If, on the other hand, a hydrogen atom present on a ligand is bound by significantly less than 55 kcal/mol, this hydrogen would be readily lost from the ligand to a neighboring sulfur bridge or to nitrogen. The only set of iron oxidation states to survive these requirements has two Fe(II) atoms in the dimer. An Fe_2(III,II) dimer binds a hydrogen atom by 65.8 kcal/mol on one of its SH ligands, and an Fe_2(I,II) dimer will lose one of its hydrogens of an SH_2 ligand at a low cost of only 42.8 kcal/mol. The only possible neutral Fe_2(II,II) dimer with one bridging sulfur and two three-coordinate iron atoms is shown in Figure 2. An indication of how this dimer model would fit into the real FeMo cofactor is shown by the dashed line in Figure 1. This is the starting dimer model for which most of the results of the present study were obtained. The symbol Fe_2(II,II) is used here, rather than Fe(II)−Fe(II), to emphasize that the oxidation states are quite delocalized over the whole complex, with significant spin populations also on sulfur. For example, the spin population on the bridging sulfur in the structure in Figure 2 is 0.27.

An important technical aspect of the calculations should be pointed out. To simplify the convergence to a proper state, ferromagnetic coupling of the spins on iron was used. In the real cluster, spins on neighboring iron atoms should in most cases be antiferromagnetically coupled, as shown by the low total spin (a quartet) of the FeMo cofactor. At least, this is most probably true for pairs of iron atoms within each cubane of the cofactor. For neighboring irons belonging to different cubanes, the situation is less clear, and these could well be ferromagnetically coupled. In previous studies on the iron dimer of MMO[27] and of manganese dimer models of photosystem II,[37] it was shown that only slightly lower energies (by a few kcal/mol) are obtained for antiferromagnetic coupling and also

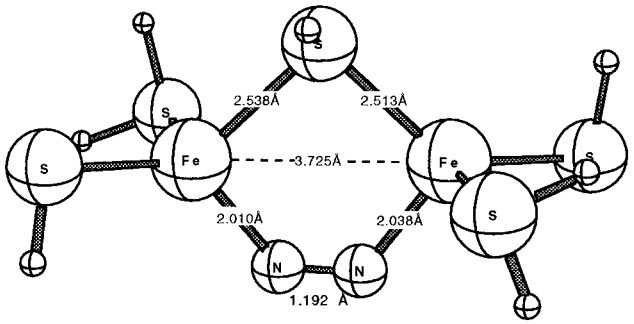

Figure 3. Reduced Fe_2(I,II) dimer with a hydrogen atom on the bridging sulfur and N_2 bound in a bridging coordination to the two irons. The sum of the binding energies of the hydrogen atom and of N_2 is 50.5 kcal/mol.

essentially identical geometries were obtained. For the present dimer model system in Figure 2, convergence was achieved also to the antiferromagnetic case and the energy is only 2.1 kcal/mol lower than for the ferromagnetic coupling. The spins on iron are 3.68 and 3.70 for the ^{9}A ferromagnetic state and 3.54 and 3.58 for the ^{1}A antiferromagnetic case. In the rest of this study only ferromagnetic coupling was used since this simplifies convergence considerably.

The most important result of the present study involves the initial steps of the ammonia formation. However, simply adding N_2 to the structure of Figure 2, was quite disappointing, because only a very weak bond is formed and every attempt to form a bridged structure failed. The only minimum found was for a structure where N_2 is end-on bonded to one of the iron atoms. The binding energy is only 0.9 kcal/mol, and the N−N distance of N_2 is exactly as in the gas phase, 1.13 Å. The present dimer model therefore does not appear to show any tendency for activation of N_2. However, as described in the Introduction, one of the key aspects of the present model for N_2-ase is that hydrogen atoms are continuously fed to the FeMo cofactor from the Fe-protein passing over the transport chain via the P-cluster. On the way to N_2, these hydrogen atoms will be bound to bridging sulfurs both on the P-cluster and on the FeMo cofactor. One such position is also present in the model dimer of Figure 2.

In a key result we find that placing a hydrogen atom on this bridging sulfur, which reduces the Fe_2(II,II) system to a Fe_2-(I,II) state, dramatically changes the affinity of the cluster for N_2. If a nitrogen molecule is now added to the cluster, the structure shown in Figure 3 is found. There are two aspects of this structure with major significance for ammonia formation by N_2-ase. First, N_2 now prefers a bridging coordination, and secondly, the N−N bond distance of 1.19 Å shows clear indications of an activated N_2. Essentially, the nitrogen has been formally reduced to the N_2^{2-} form. A problem of reaching the structure in Figure 3 is that the binding energy obtained by adding the hydrogen atom to the bridging sulfur in the structure in Figure 2 is very low, only 18.6 kcal/mol. There are many positions in the neighborhood in the FeMo cofactor that bind hydrogen much better, but the structure in Figure 3 could still be accessible in the following way. Initially, N_2 could be bound end-on to one of the iron atoms with a small binding energy, as described above. If one hydrogen atom now binds to the bridging sulfur, the N_2 molecule could simultaneously move to a bridge-bonding situation as in Figure 3. The sum of the binding energies of both the hydrogen and N_2 together is then 50.5 kcal/mol, in line with our earlier estimate of a reaction energy for each step of the ammonia synthesis of 50−60 kcal/mol. The S−H bond formation in Figure 3 is considered to be critical for ammonia synthesis by N_2-ase and is also discussed for the larger models in the next subsection.

TABLE 1: Binding Energies (kcal/mol) for H on N_2 ($D(H_N)$), H on the Bridging S ($D(H_S)$), and N_2 to the Cluster ($D(N_2)$) Using the Dimer Model (Structures 1−8 in Scheme 1) and B3LYP/6311+G(2d,2p)

structure	$D(H_N)$	$D(H_S)$	$D(N_2)$
1a (HS)(H_2S)Fe−S−Fe−(SH)SH_2)			
2a (HS)(H_2S)Fe−N_2−S−Fe−(SH)SH_2)			−0.9
3a (HS)(H_2S)Fe−N_2H−S−Fe−(SH)SH_2)	−22.7		
4a (HS)(H_2S)Fe−N_2H_2−S−Fe−(SH)SH_2)	−73.9		
5a (HS)(H_2S)Fe−N_2H_3−S−Fe−(SH)SH_2)	−76.1		
6a (HS)(H_2S)Fe−N_2H_4−S−Fe−(SH)SH_2)	−79.8		
7a (HS)(H_2S)Fe−NH_2−S−Fe−NH_3−(SH)SH_2)	−65.8		
8a (HS)(H_2S)Fe−NH_3−S−Fe−NH_3−(SH)SH_2)	−108.1		
1b (HS)(H_2S)Fe−SH−Fe−(SH)SH_2)		−18.6	
2b (HS)(H_2S)Fe−N_2−SH−Fe−(SH)SH_2)		−49.6	−31.9
3b (HS)(H_2S)Fe−N_2H−SH−Fe−(SH)SH_2)	−48.1	−78.6	
4b (HS)(H_2S)Fe−N_2H_2−SH−Fe−(SH)SH_2)	−73.8	−78.5	
5b (HS)(H_2S)Fe−N_2H_3−SH−Fe−(SH)SH_2)	−66.9	−69.3	
6b (HS)(H_2S)Fe−N_2H_4−SH−Fe−(SH)SH_2)	−56.2	−45.7	
7b (HS)(H_2S)Fe−NH_2−SH−Fe−NH_3(SH)SH_2)	−121.1	−101.1	
8b (HS)(H_2S)Fe−NH_3−SH−Fe−NH_3(SH)SH_2)	−53.1	−46.1	

The electronic structure of the complexes in Figures 2 and 3 can be described in the following way. First, the dimer model in Figure 2 can be characterized as quite strongly delocalized Fe_2(II,II) with spin populations of 3.68 and 3.70 on the irons and 0.27 on the bridging sulfur. The SH ligands have spins of 0.13 and 0.10 each, while the spins on the SH_2 ligands are quite small. It should be remembered that these SH and SH_2 ligands represent the totality of the FeMo cofactor, not only the bridging sulfurs but also the other iron atoms, and are used mainly to get an appropriate oxidation state for the iron atoms in the model. When a hydrogen atom is bound to the bridging sulfur, it reduces the spin on this sulfur from 0.27 to 0.05. But, more importantly, it also promotes the iron atoms and gives them partial Fe(I) character. The spin-change on the irons from 3.70/3.68 to 3.39/3.30 is indicative of some promotion which leads to a quite different binding of N_2 than before hydrogen addition to the bridging sulfur. Their higher d-population allows the irons to donate significant electron density to N_2, which leads to some covalent Fe−N bond formation and an elongation of the N−N bond from 1.13 Å to 1.19 Å. In this process the iron spins change from 3.39/3.30 to 3.56/3.54, and the spin on nitrogen becomes −0.29 and −0.30. Thus, the spins on iron and nitrogen have opposite signs and are rather large on nitrogen, indicating weak covalent bonding.

The cooperative binding of a hydrogen atom on a bridging sulfur and of a nitrogen molecule in a bridging position is the key point that dictated how the remaining steps of the ammonia formation were studied. In what follows, the results of adding hydrogen atoms to N_2 are obtained in parallel for both the case where the bridging sulfur binds a hydrogen atom and when it does not, with results shown in Table 1. The corresponding spin populations are given in Table 2.

One of the most puzzling facts concerning ammonia synthesis by N_2-ase is that one hydrogen molecule is formed for every N_2 consumed. In light of the above result that a hydrogen atom on a bridging sulfur is critical for the activation of N_2, it is tempting to draw the conclusion that this hydrogen is half of the H_2 molecule formed. However, before this is done larger models need to be tested. Some additional information concerning the role of hydrogen atoms on larger clusters will be given in the next subsection.

A few calculations were performed to investigate the potential surface in the region around the bridging N_2 minimum. In particular, a possible barrier to reach the minimum cannot be

TABLE 2: Spin Population on Fe, N, and the Bridging S Using the Dimer Model (Scheme 1). The Atoms Are Numbered from "Left" to "Right" in the Structures of Scheme 1

	structure	S	Fe1	Fe2	N1	N2
1a	$(HS)(H_2S)Fe-S-Fe-(SH)SH_2$)	0.27	3.70	3.67		
1b	$(HS)(H_2S)Fe-SH-Fe-(SH)SH_2$)	0.06	3.30	3.39		
2a	$(HS)(H_2S)Fe-N_2-S-Fe-(SH)SH_2$)	0.33	3.64	3.68	0.04	−0.05
2b	$(HS)(H_2S)Fe-N_2-SH-Fe-(SH)SH_2$)	0.10	3.56	3.54	−0.29	−0.30
3a	$(HS)(H_2S)Fe-N_2H-S-Fe-(SH)SH_2$)	0.31	3.68	3.49	−0.26	−0.58
3b	$(HS)(H_2S)Fe-N_2H-SH-Fe-(SH)SH_2$)	0.15	3.66	3.61	−0.03	0.20
4a	$(HS)(H_2S)Fe-N_2H_2-S-Fe-(SH)SH_2$)	0.57	3.77	3.77	−0.35	−0.35
4b	$(HS)(H_2S)Fe-N_2H_2-SH-Fe-(SH)SH_2$)	0.13	3.64	3.64	−0.42	−0.42
5a	$(HS)(H_2S)Fe-N_2H_3-S-Fe-(SH)SH_2$)	0.60	3.85	3.69	0.29	0.00
5b	$(HS)(H_2S)Fe-N_2H_3-SH-Fe-(SH)SH_2$)	0.15	3.64	3.67	0.18	0.00
6a	$(HS)(H_2S)Fe-N_2H_4-S-Fe-(SH)SH_2$)	0.35	3.65	3.65	0.01	0.01
6b	$(HS)(H_2S)Fe-N_2H_4-SH-Fe-(SH)SH_2$)	0.14	3.29	3.38	0.00	0.01
7a	$(HS)(H_2S)Fe-NH_2-S-Fe-NH_3-(SH)SH_2$)	−0.38	3.45	3.70	0.19	0.00
7b	$(HS)(H_2S)Fe-NH_2-SH-Fe-NH_3(SH)SH_2$)	0.17	3.71	3.69	0.03	0.07
8a	$(HS)(H_2S)Fe-NH_3-S-Fe-NH_3-(SH)SH_2$)	0.41	3.61	3.62	0.03	0.03
8b	$(HS)(H_2S)Fe-NH_3-SH-Fe-NH_3(SH)SH_2$)	0.10	3.29	3.31	0.03	0.02

automatically excluded. However, geometry optimizations starting with N_2 quite far away from the minimum in Figure 3 led back to this minimum without any barrier. Furthermore, a geometry optimization was started at the minimum of Figure 3 but with removal of the hydrogen atom at the bridging sulfur. Convergence was then achieved to the weak end-on minimum described above without any barrier, showing that a bridging N_2 coordination is not even a local minimum without the hydrogen on the bridging sulfur.

Finally, all of the results given in Table 1 should be discussed together to see how well this simple dimer model reproduces the ideal situation that in each step nitrogen should bind hydrogen atoms by 50−60 kcal/mol. Since the first hydrogen atom ends up on the bridging sulfur, the second hydrogen atom is the first that binds to N_2. As shown above by the gas-phase values, this is a quite critical step. Again, the presence of the hydrogen on the bridging sulfur is quite important. Without the hydrogen, the energy gain in this step would be only 22.7 kcal/mol, very far from the ideal 50−60 kcal/mol. In fact, this binding energy is so low that the hydrogen atom would never stay on nitrogen but proceed to some other place. However, with the hydrogen atom on the sulfur, the binding energy of the hydrogen atom on nitrogen is 48.1 kcal/mol, which is at least reasonably in line with the optimal 50−60 kcal/mol, considering the simplicity of the dimer model. The spin on the N_2H unit is 0.17, which is substantially smaller than 0.59 obtained for the N_2 unit in the previous step. This is not surprising since the covalency of the N−H bond is much more dominant than in the Fe−N bond.

The next step in the ammonia cycle is N_2H_2 formation, which should not be a critical step since the reaction is already exothermic by 62.0 kcal/mol in the gas phase. Indeed, the addition of the second hydrogen to nitrogen is exothermic by 73.9 kcal/mol without, and by 73.8 kcal/mol with, a hydrogen bound to the bridging sulfur. Since this is above the optimal 50−60 kcal/mol, however, some energy might be wasted in this step. The N−N distance increases in this step to 1.36 Å, indicating that most of the N−N π-bonding is lost. The weak covalency in the Fe−N bonds leads to large negative spin-populations of −0.42 on the nitrogens, similar to the situation where the N_2 molecule was initially bound; see above. The next two steps forming N_2H_3 and N_2H_4 are not critical either. Formation of N_2H_3 is exothermic by 76.1 kcal/mol without and by 66.9 kcal/mol with hydrogen on sulfur, while formation of N_2H_4 has exothermicities of 79.8 and 56.2 kcal/mol, respectively. It can be noted that the hydrogen on the bridging sulfur makes both these energies better in line with the optimal 50−60 kcal/mol. Without this hydrogen some energy would be wasted. Summarizing the situation up to this pont, it can be concluded that with a hydrogen bound to the bridging sulfur the reaction exothermicities of each addition of hydrogen fulfills the requirement of being in the range 50−60 kcal/mol remarkably well for such a simple model of N_2-ase. The exothermicities are 50.5 kcal/mol (combined hydrogen and N_2 addition to the structure in Figure 2), 48.1 kcal/mol, 73.8 kcal/mol, 66.9 kcal/mol, and 56.2 kcal/mol, for the first five hydrogen atoms added to the cluster (where one hydrogen atom ends up at the sulfur bridge).

At the stage where N_2H_4 is formed, a new situation is reached where the simple dimer model may not be able to adequately represent the situation of the actual cluster as well as it does for the first steps. N_2H_4 is a relatively stable molecule and could, for example, start to diffuse in the actual cluster. It is also rather big, and the empty space around the site where the initial hydrogen attacks occur may not be sufficient to harbor it. Although very speculative at this stage, one possible scenario is the following. The first hydrogen that reaches the active site of the cluster combines with the hydrogen on the bridging sulfur to form H_2. Since the energy for this step is as large as 65.5 kcal/mol, well above the average energy for each step of ammonia formation of 50−60 kcal/mol, formation of H_2 at this point is quite possible. Since N_2H_4 is sufficiently loosely bound to the iron dimer, it can then possibly move to the surface of the cofactor. The next hydrogen atom reaching the nitrogens would then form one NH_3 and one NH_2, bound to separate irons. The energy for this step is, as seen from the left column of Table 1, 65.8 kcal/mol. In the final step, an incoming hydrogen atom completes the formation of also the second ammonia. As seen from Table 1, this step is computed to be very exothermic by 108.1 kcal/mol, far outside the optimal 50−60 kcal/mol. There could be two reasons for this large energy gain. The first one is that the model dimer is simply not a good model for the final steps of ammonia formation. An indication of this is that rather than forming a weak bond to ammonia, the dimer starts to lose an H_2S ligand. This can, of course, not happen in the actual cluster, where all sulfurs are μ-oxo bound, and it is therefore possible that the calculations overestimate the energy gain in this step. The second reason for the large energy gain in the final step is that this energy is needed to evaporate ammonia from the cluster. Only more realistic model calculations including the entire cofactor in the model will show if these speculations have some truth in them.

At the end of the present study, several alternative possibilities for the structures in Scheme 1 were investigated. Only one

SCHEME 1: Structures Obtained for the Dimer Model. The a Structures Have a Bridging Sulfur, While the b Structures Have an Additional Hydrogen Atom on This Sulfur

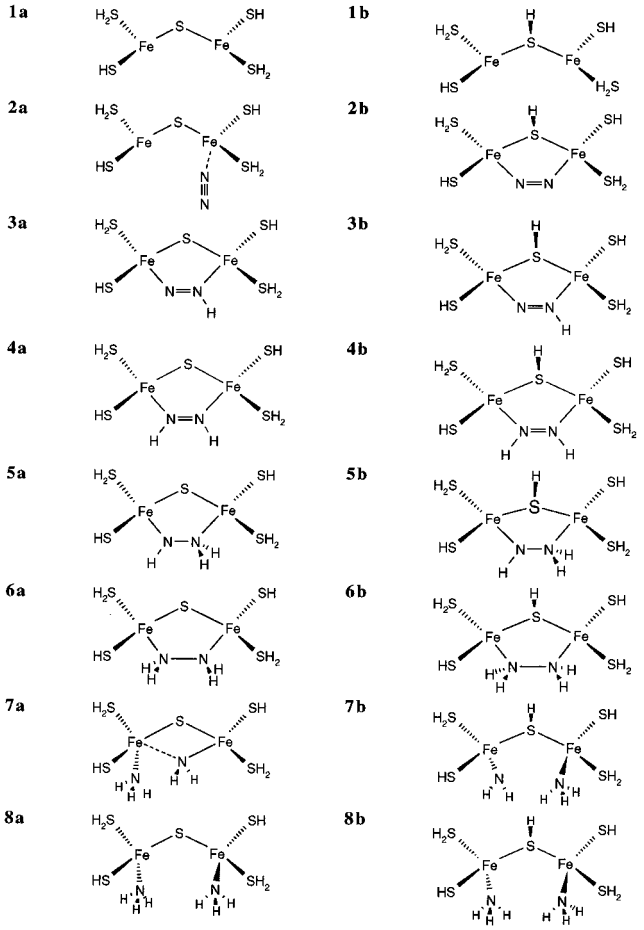

such structure could be of interest and this concerns structure **1b**. The local promotion effect due to the hydrogen added to the bridging sulfur makes it possible to form a structure with significant Fe−Fe bonding. This type of bonding does not occur for structure **1a**. The Fe−Fe-bonded structure of **1b** is as much as 37.4 kcal/mol more stable than without Fe−Fe bonding. This result means that the addition of the first hydrogen becomes exothermic by 55.9 kcal/mol rather than 18.5 kcal/mol. Since Fe−Fe bonding does not occur for any other structure, such as for **2b**, it has no effect on the combined binding energy of the first hydrogen atom and N_2. It only affects the order the first hydrogen atom and N_2 bind to the cluster. If Fe−Fe bonding is a true representation of the real situation, the hydrogen atom will first bind to the cluster and then N_2. If Fe−Fe bonding is an artifact of the model, N_2 will bind first with a weak binding energy, as discussed above. No other steps discussed above are affected. The possible significance of Fe−Fe bonding will be investigated further in a coming study.

b. Larger Models for N_2-ase. The actual FeMo cofactor, see Figure 1, can be considered to be built up from two incomplete M_4S_3 cubanes, each one with a missing sulfur. In one of these cubanes the metals are all iron, while in the other one there is one molybdenum. The two cubanes are linked by three sulfur bridges, which help hold the cluster together. All but one of the irons are three-coordinate, while molybdenum is six-coordinate. In the present subsection some results will be presented for models that approach this actual FeMo cofactor, in an attempt to test the significance of the results obtained for

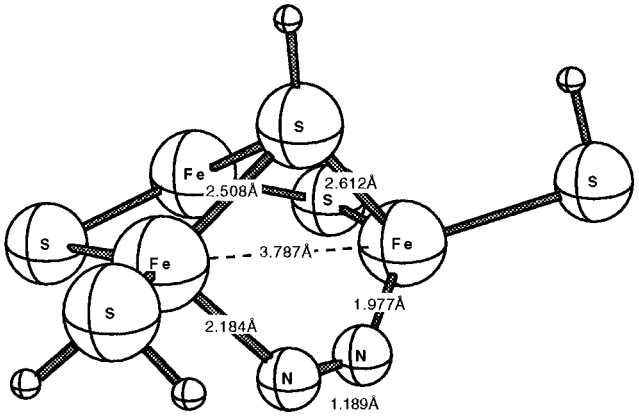

Figure 4. Trimer model with a bridging SH group and N_2 coordinated in a similar way as in the dimer model (Figure 3). The sum of the binding energies of the hydrogen atom and of N_2 is 47.1 kcal/mol.

the dimer model discussed above. The main interest will be focused on the activation of N_2 and the possible role in this process of hydrogen atoms bound to sulfur bridges. The largest model used here is an Fe_8S_9 cluster where an iron has replaced the actual molybdenum in order to achieve a higher symmetry in the calculations.

In the first extension of the dimer model, an iron trimer cluster was used; see Figure 4. The SH and SH_2 ligands in this model were again chosen to make all irons Fe(II), keeping the cluster neutral. The main goal with the trimer model is to test whether the presence of μ^3 sulfurs makes a difference compared to the μ^2 bridge used for the dimer model. An N_2 molecule and a hydrogen atom are then added to the trimer model exactly like what was done for the dimer model. As seen in Figure 4, the structure is now quite similar to the one found for the dimer shown in Figure 3. The sum of the binding energies of the hydrogen atom on the sulfur bridge and of N_2 is rather similar in the dimer and trimer model, being 3.4 kcal/mol smaller for the trimer using the small basis set. Extrapolated to the large basis set, this gives a binding energy for the trimer of 47.1 kcal/mol. Both models also show a strongly activated N_2 with an N−N bond length of 1.19 Å. In summary, the dimer and trimer models show clear similarities.

In the next extension, two different models with four iron atoms are used. In the first of these an incomplete Fe_4S_3 cluster is used, corresponding to half of the FeMo cofactor. Again, SH and SH_2 ligands were added to keep three-coordination with only Fe(II) atoms present. Adding a hydrogen atom and a bridging N_2 as in Figure 5 leads to a quite similar structure as the ones for the dimer and the trimer with an activated N_2 with an N−N distance of 1.19 Å. However, the sum of the binding energies of the hydrogen atom and of N_2 is now substantially smaller by 18.5 kcal/mol compared to the dimer using the small basis set. Extrapolation to the large basis set gives a binding energy for this cluster of only 32.0 kcal/mol, far from the optimal 50−60 kcal/mol. The conclusion tentatively drawn is that N_2 might prefer to bind across the two cubane clusters of the FeMo cofactor rather than to just one of them.

To see if the missing sulfur in the corner of the cubanes is a significant feature, a complete cubane Fe_4S_4 cluster was also tried. This cluster is similar to the ones found in the P-cluster, but in the Fe_4S_4 model the irons are kept three-coordinate as in the FeMo cofactor. The cluster was kept neutral, which again means only Fe(II) atoms are present. In this case the addition of a hydrogen atom and a bridging N_2 did not lead to an activated N_2. N_2 simply moved from the bridging position and formed a weak end-on bond to one of the iron atoms, showing

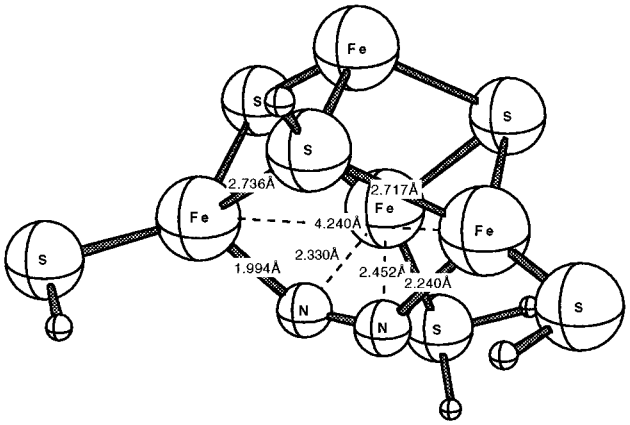

Figure 5. Tetramer model with a bridging SH group and N_2 coordinated in a similar way as in the dimer model (Figure 3). The sum of the binding energies of the hydrogen atom and of N_2 is 32.0 kcal/mol.

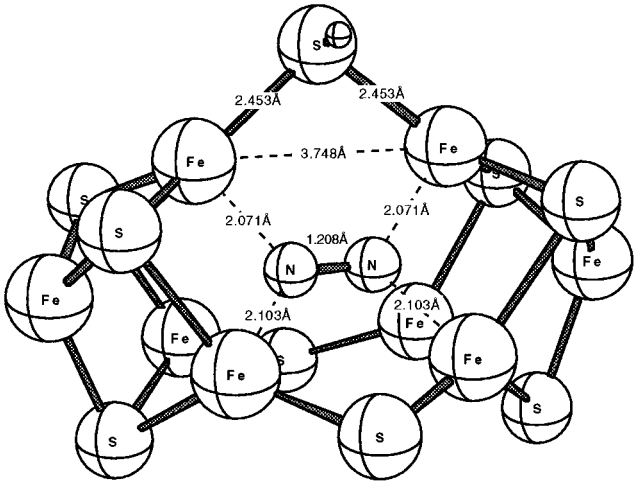

Figure 6. $Fe_8S_9^{2-}$ model with a bridging SH group and N_2 coordinated in a similar way as in the dimer model (Figure 3). The sum of the binding energies of the hydrogen atom and of N_2 is 46.5 kcal/mol.

that a missing sulfur position in the cubane structure could be an essential factor in N_2 activation.

In the final models tried, a cluster quite similar to the actual FeMo cofactor (see Figure 1) was used with eight iron atoms and nine sulfur atoms. An iron atom replaced the molybdenum atom to increase the symmetry. No additional ligands were added, and ferromagnetic coupling was used. As a starting point for these studies all iron atoms were kept in oxidation state II, as in the smaller models, even though some Fe(III) character is known to be present in the real cofactor. Two different ways of obtaining a cluster with all Fe(II) atoms were used. In the first, the cluster was simply charged to become $Fe_8S_9^{2-}$. C_s symmetry was kept, and N_2 was placed inside the cavity between the cubanes. This led to a very repulsive interaction. If, on the other hand, one hydrogen atom is placed on a sulfur bridging the two cubanes and N_2 is placed bridging these same irons (see Figure 6) as for the smaller cluster models, the interaction is found to be attractive. The sum of the binding energies of the hydrogen atom on the bridging sulfur and of N_2 is 4.0 kcal/mol smaller than obtained for the dimer and only 0.6 kcal/mol smaller than for the trimer, using the same basis sets. Extrapolated to the large basis set, this leads to a binding energy of H and N_2 for the $Fe_8S_9^{2-}$ cluster of 46.5 kcal/mol. It should be noted that the binding energy should increase somewhat for the large cluster if the symmetry constraint is released. The remarkable similarity of these results, considering the simplicity

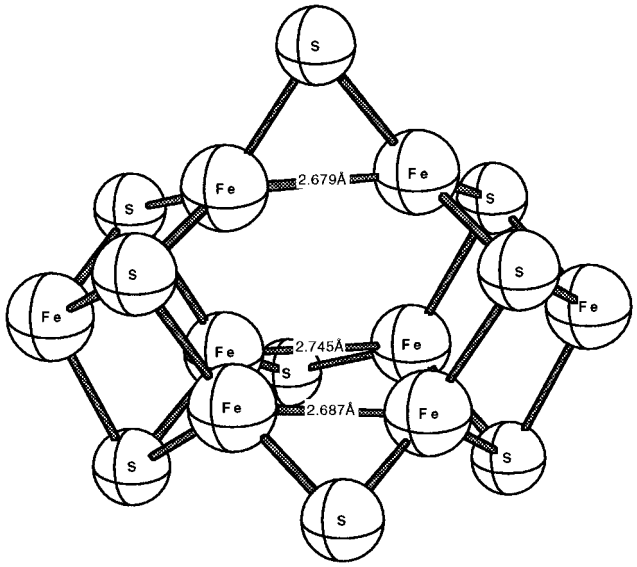

Figure 7. Neutral Fe_8S_9 model with six Fe(II) and two Fe(III) atoms.

of the models, shows that the hydrogen promotion effect to a large extent is independent of cluster size, and this promotion effect is thus one of the most important results of the present study. The N−N distance of 1.21 Å is also similar to the result of 1.19 Å obtained for the smaller clusters, but the coordination mode is somewhat different. In the $Fe_8S_9^{2-}$ cluster N_2 is four-coordinate rather than two-coordinate, but again it should be emphasized that C_s symmetry was enforced for the large cluster. A notable feature of the naked cluster (without the added hydrogen atom and N_2) is that the Fe−Fe distance between the two cubanes is much larger than found in the X-ray structure, 3.3 Å compared to only 2.4−2.6 Å. This artifact is present also for the second model of an all-Fe(II) cluster, where the cluster is kept neutral by replacing two of the sulfur bridges between the two cubanes by bridging SH groups. In this case the Fe−Fe distance between the cubanes is as large as 3.7 Å (no d-functions on sulfur were used; see below). Apart from the fact that this distance probably is very sensitive to the detailed description of the cluster and does not contain much energy, the distance could depend on the oxidation states of the iron atoms. An indication of the sensitivity of the results can be obtained by results for different basis sets. The above result for the $Fe_8S_9^{2-}$ cluster was in fact obtained with d-functions on sulfur. For the smaller dimer model the effect of these d-functions was a decrease of the Fe−Fe distance by as much as 0.6 Å. The sensitivity to the choice of oxidation states was tested by going to a model with two Fe(III) atoms in the cluster. This situation is achieved by making the $Fe_8S_9^{2-}$ cluster neutral (see Figure 7), which led to a significant shortening of the Fe−Fe distance between the cubanes down to a value of 2.7 Å, in quite good agreement with the X-ray structure. Apparently, the introduction of higher oxidation states has led to the formation of some weak Fe−Fe bonding between the cubane units.

The above result concerning the dependence of the distance between the cubanes on the oxidation states leads to interesting possibilities. In particular, the results show that the neutral Fe_8S_9 cluster with two Fe(III) atoms gives a closed cavity inside the cluster with too short Fe−Fe distances for N_2 to be able to enter. When two hydrogen atoms are placed on the bridging sulfurs between the cubanes, giving a cluster with all Fe(II) atoms, the cavity opens up and allows N_2 to enter. It is interesting to note that the FeMo cofactor has been found to be reduced in three steps before N_2 is activated and N−H bonds start to be formed.[4]

Some of this reduction could be associated with opening up the cavity for N_2. Likewise, the formation of H_2 could be a result of closing the cavity again by removing the hydrogens on the bridges. This is, of course, very speculative at this early stage but could be a useful starting point for further studies of more realistic models and also for more detailed studies.

IV. Conclusions

The present study is the first of a series of studies on the mechanism for ammonia formation by nitrogenase. In this initial study, it has been considered of most importance to obtain general ideas of what might be the main factors responsible for the activation of N_2 and for the subsequent formation of the N−H bonds. For this reason a model as simple as possible was chosen. The neutral Fe_2(II,II) dimer model has indeed given some interesting new information concerning ammonia synthesis probably relevant also for the actual FeMo cofactor. The most important result obtained is that hydrogen atoms play significant roles not only by binding to N_2 but also by binding to the bridging sulfurs of the cluster. For the dimer it was found absolutely critical to bind a hydrogen atom to the bridging sulfur to get these iron atoms to activate N_2. Preliminary tests of this result for larger clusters show that the same effect is present also in these cases. For the largest cluster another interesting effect was noted. It was found that the access to the cavity inside the cluster between the cubanes could be regulated by the oxidation states on the irons. With two Fe(III) atoms the cavity was found to be closed for N_2. Adding two hydrogen atoms on the bridging sulfurs between the cubanes, making all iron atoms Fe(II), opens up the cavity for easy access of N_2. Although the mechanism is not clear at this stage, it is tempting to suggest that these hydrogen atoms necessary for the chemistry of N_2-ase are also the ones that form the H_2 molecule produced for every N_2 activated.

Simple energetic arguments have also been an important guideline for the present study. It is argued on the basis of gas-phase energetics that hydrogen atoms need to be produced by the Fe-protein with an energy in the range 50−60 kcal/mol. A similar energy range should also apply for the addition of hydrogen atoms to the FeMo cofactor in each step of the ammonia synthesis. The model calculations on the iron dimer confirm this suggestion. The computed exothermicities for the first five steps are 50.5, 48.1, 73.8, 66.9, and 56.2 kcal/mol, where the hydrogen atom in the first step ends up on a bridging sulfur. In this simple model some energy would thus be wasted in steps three and four, but some loss of energy might be necessary also for the actual enzyme. As N_2H_4 is formed, the dimer model may no longer be a reasonable model. Too much energy, far outside the ideal 50−60 kcal/mol, is produced as ammonia is formed in the final steps using this model. However, it is possible that some of this excess energy could be used to expel ammonia from the cofactor. Clearly, as more information and suggestions of this type become available, the need to do more realistic calculations on the cofactor increases. Such calculations are planned for the near future and will be presented in later papers.

References and Notes

(1) Ludden, P. W. *Encyclopedia of Inorganic Chemistry*; Wiley: New York, 1994; p 2566.

(2) Coucouvanis, D. *Encyclopedia of Inorganic Chemistry*; Wiley: New York, 1994; p 2557.

(3) Howard, J. B.; Rees, D. C. *Chem. Rev.* **1996**, *96*, 2965.

(4) Burgess, B. K.; Lowe, D. J. *Chem. Rev.* **1996**, *96*, 2983.

(5) Eady, R. R. *Chem. Rev.* **1996**, *96*, 3013.

(6) Orme-Johnson, W. H. *Annu. Rev. Biophys. Chem.* **1985**, *14*, 419.

(7) Stiefel, E. I.; Thomann, H.; Jin, H.; Bare, R. E.; Morgan, T. V.; Burgmayer, S. J. N.; Coyle, C. L. *Metal Clusters in Proteins*; Que, L., Ed.; American Chemical Society: Washington, DC, **1988**; p 372.

(8) Smith, B. E.; Eady, R. R. *Eur. J. Biochem.* **1992**, *205*, 1.

(9) Carnahan, J. E.; Mortensen, L. E.; Mower, H. F.; Castle, J. E. *Biochim. Biophys. Acta* **1960**, *44*, 520.

(10) Hardy, R. W. F.; Burns, R. C.; Parshall, G. W. *Adv. Chem. Ser.* **1971**, *100*, 219.

(11) Eady, R. R. *Perspectives on Bioinorganic Chemistry*; JAI Press: Greenwich, CT, 1991; p 255.

(12) Bishop, P. E.; Joerger, R. D. *Annu. Rev. Plant. Physiol. Plant Mol. Biol.* **1990**, *41*, 109.

(13) Kim, J.; Rees, D. C. *Nature* **1992**, *360*, 553.

(14) Dean, D. R.; Bolin, J. T.; Zheng., L. *J. Bacteriol.* **1993**, *175*, 6737.

(15) Shah, V. K.; Brill. *Proc. Natl. Acad. Sci.* **1977**, *74*, 3249.

(16) Thorneley, R. N. F.; Lowe, D. J. *Molybdenum Enzymes*; Spiro, T., Ed.; Wiley: New York, 1985; p 221.

(17) Liang. J.; Burris, R. H. *Proc. Natl. Acad. Sci.* **1988**, *85*, 9446.

(18) Kim, J.; Rees, D. C. *Science* **1992**, *257*, 1677.

(19) Crabtree, R. H.; Hlatky, G. G. *J. Organomet. Chem.* **1982**, *C21*−*C23*, 238.

(20) Chan, M. K.; Kim, J.; Rees, D. C. *Science* **1993**, *260*, 792.

(21) Deng, H. B.; Hoffmann, R. *Angew. Chem., Int. Ed. Engl.* **1993**, *32*, 1062.

(22) Zerner, M. C.; Stavrev, K. K. *Chem. Eur. J.* **1996**, *2*, 83.

(23) Dance, I. *Chem. Commun.* **1997**, 165.

(24) Becke, A. D. *Phys. Rev.* **1988**, *A38*, 3098. Becke, A. D. *J. Chem. Phys.* **1993**, *98*, 1372. Becke, A. D. *J. Chem. Phys.* **1993**, *98*, 5648.

(25) Bauschlicher, Jr.; Partridge, H. *Chem. Phys. Lett.* **1995**, *240*, 533.

(26) Blomberg, M. R. A.; Siegbahn, P. E. M.; Svensson, M. *J. Chem. Phys.* **1996**, *104*, 9546.

(27) Siegbahn, P. E. M.; Crabtree, R. H. *J. Am. Chem. Soc.* **1997**, *119*, 3103.

(28) Shu, L.; Nesheim, J. C.; Kauffmann, K.; Munck, E.; Lipscomb, J. D.; Que, L., Jr. *Science* **1997**, *275*, 515.

(29) Siegbahn, P. E. M.; Blomberg, M. R. A.; Crabtree, R. H. *Theor. Chem. Acc.* **1997**, *97*, 289.

(30) Thorneley R. N. F. In *New Horizons in Nitrogen Fixation*; Palacias, R., Ed.; Kluwer: Dordrecht, 1993; p 79.

(31) Frisch, M. J.; Trucks, G. W.; Schlegel, H. B.; Gill, P. M. W.; Johnson, B. G.; Robb, M. A.; Cheeseman, J. R.; Keith, T.; Petersson, G. A.; Montgomery, J. A.; Raghavachari, K.; Al-Laham, M. A.; Zakrzewski, V. G.; Ortiz, J. V.; Foresman, J. B.; Cioslowski, J.; Stefanov, B. B.; Nanayakkara, A.; Challacombe, M.; Peng, C. Y.; Ayala, P. Y.; Chen, W.; Wong, M. W.; Andres, J. L.; Replogle, E. S.; Gomperts, R.; Martin, R. L.; Fox, D. J.; Binkley, J. S.; Defrees, D. J.; Baker, J.; Stewart, J. P.; Head-Gordon, M.; Gonzalez, C.; Pople, J. A. *Gaussian 94 Revision B.2*; Gaussian Inc.: Pittsburgh, PA, 1995.

(32) Stevens, P. J.; Devlin, F. J.; Chablowski, C. F.; Frisch, M. J. *J. Phys Chem.* **1994**, *98*, 11623.

(33) Lee, C.; Yang, W.; Parr, R. G. *Phys. Rev.* **1988**, *B37*, 785.

(34) Vosko, S. H.; Wilk, L.; Nusair, M. *Can. J. Phys.* **1980**, *58*, 1200.

(35) Perdew J. P.; Wang, Y. *Phys. Rev. B* **1992**, *45*, 13244. Perdew, J. P. In *Electronic Structure of Solids*; Ziesche, P., Eischrig, H., Eds.; Akademie Verlag: Berlin, 1991. Perdew, J. P.; Chevary, J. A.; Vosko, S. H.; Jackson, K. A.; Pederson, M. R.; Singh, D. J.; Fiolhais, C. *Phys. Rev. B* **1992**, *46*, 6671.

(36) Hay, P. J.; Wadt, W. R. *J. Chem. Phys.* **1985**, *82*, 299.

(37) Blomberg, M. R. A.; Siegbahn, P. E. M.; Styring, S.; Babcock, G. T.; Åkermark, B.; Korall, P. *J. Am. Chem. Soc.* **1997**, *119*, 8285.